The role of the subtropical jet in deficient winter precipitation across the mid-Holocene Indus basin

Article

Accepted Version

To link to this article DOI: http://dx.doi.org/10.1029/2019GL081920

Publisher: American Geophysical Union

The role of the subtropical jet in deficient winter precipitation across the mid-Holocene Indus basin

K. M. R. Hunt[1,2], **A. G. Turner**[1,2]

[1]Department of Meteorology, University of Reading, United Kingdom
[2]National Centre for Atmospheric Science, University of Reading, United Kingdom

Key Points:

- Greater seasonality during the mid-Holocene reduces temperature gradient and weakens the subtropical jet in northern hemisphere winter. (135 chars)
- Weaker and less frequent western disturbances reach South Asia, leading to a 15% fall in winter precipitation in the Indus Basin. (129 chars)
- The known stronger summer monsoon combined with reduced winter rainfall gives a striking shift in seasonality in the mid-Holocene. (130 chars)

Corresponding author: Kieran M. R. Hunt, `k.m.r.hunt@reading.ac.uk`

Abstract

The mid-Holocene (7-5 ka) was a period with an increased seasonal insolation cycle, resulting from decreased insolation during northern hemisphere winter. Here, a set of six CMIP5 models is used to show that the decreased insolation reduced the upper-tropospheric meridional temperature gradient, producing a weaker subtropical jet with less horizontal shear.

These effects work to reduce the baroclinic and barotropic instability available for perturbations to grow, and in consequence, storm-tracking results show that there are fewer winter storms over India and Pakistan (known as western disturbances). These western disturbances are weaker, resulting in a reduction in winter precipitation of around 15% in the north Indus Basin.

Combined with previous work showing greater northwestward extent of the Indian monsoon during the mid-Holocene, our GCM-derived results are consistent with the Indus Basin changing from a summer-growing season in the mid-Holocene to a winter-growing season in the present day.

1 Introduction

The subtropical westerly jet (STWJ) is a quasi-permanent feature of the Eurasian upper troposphere (Krishnamurti, 1961), a thermal wind brought about by a strong meridional temperature gradient. It exhibits a distinctive seasonal cycle in latitude: at Indian longitudes during the boreal summer, it is at approximately 25°N, moving north of the Tibetan Plateau during the monsoon to about 45°N (Schiemann, Lüthi, & Schär, 2009). Embedded within the STWJ are numerous eddies, which intensify in the baroclinically unstable environment on approach to India and Pakistan (Hunt, Curio, Turner, & Schiemann, 2018), where they become known as western disturbances (WDs). WDs are responsible for a large majority of winter rainfall in Pakistan and north India (Hunt, Turner, & Shaffrey, 2019; Martyn, 2002; Syed, Giorgi, Pal, & King, 2006), a region thoroughly dependent on winter agriculture.

The mid-Holocene (∼7-5 ka; taken as 6 ka for simulations) is the name given to the warm period that occurred during the middle of the current interglacial; orbital precession, with minor contributions from increased orbital obliquity and eccentricity resulted in a stronger seasonal cycle and a shallower meridional temperature gradient (e.g. Bosmans et al., 2012; Harrison et al., 2003). As a result, both proxies and climate models suggest that the South Asian monsoon had a greater magnitude and deeper northwestward extent during this period (Braconnot et al., 2002, 2007; Bryson & Swain, 1981; Joussaume et al., 1999; Liu, Harrison, Kutzbach, & Otto-Bliesner, 2004; Rawat, Gupta, Srivastava, Sangode, & Nainwal, 2015).

The end of the mid-Holocene (MH) period marked the economic and social collapse of a large civilisation in the Indus basin, the so-called Harappan Civilisation (Misra, 1984; Possehl, 1997a, 1997b). Authors have attributed this to variety of possibly connected causes: the drying up of important Indus tributaries (e.g. Dikshit, 1979), rerouting of tributaries (Raikes & Dales, 1986), changing flood hazards (Flam, 2002), and changing seasonality of the river discharge available for irrigation (Giosan et al., 2012). These are typically attributed to the contemporaneous and permanent withdrawal of the summer monsoon from the region (Berkelhammer et al., 2012; Staubwasser, Sirocko, Grootes, & Segl, 2003), as described above.

Even so, reviewing authors have long argued the need to consider the changes in annual precipitation to the region (Bryson & Swain, 1981; Pant & Maliekal, 1987; Raikes & Dyson, 1961) given the significant contribution of WDs to the present-day climate. Bryson (1997) noted, however, that winter rainfall proxies for the region (e.g. Bryson, 1992) are not only sparse but, when used to assess the difference between mid-Holocene and present day precipitation, fail to agree in sign let alone magnitude and pointed out the need for further research on the topic, which thus far has not been conclusive (Madella & Fuller, 2006). Recent isotopic modelling work (J. Li et al., 2017) indicated that precipitation proxies did not agree in the nearby Tibetan Plateau.

Nevertheless, this region is capable of trends of measurable magnitude, as seen in recent observations (You et al., 2017). Palazzi, Hardenberg, and Provenzale (2013); Palazzi, von Hardenberg, Terzago, and Provenzale (2015) showed that in both present-day CMIP5 experiments and observations, the seasonal cycle shifts from summer-dominated (monsoonal) precipitation in the central and eastern Himalaya to winter-dominated (western disturbance) precipitation in the western Himalaya and Karakoram. Thus, if the summer monsoon had a more westward extent during the mid-Holocene, we would expect important changes to the seasonal cycle in this region.

So, previous studies have established that the summer monsoon extended further into the Indus basin during the mid-Holocene, and that this is a region that contains a transition in the seasonal cycle of precipitation. It is not clear, however, what happened to the boreal winter STWJ during the mid-Holocene – and thus how western disturbances were affected; though some authors (Hou, D'Andrea, Wang, He, & Liang, 2017; Wei & Wang, 2004) have noted that the summer STWJ was climatologically further north in the mid-Holocene. Here, we seek to quantify and understand how the jet behaves in CMIP5 simulations of the mid-Holocene, before using a tracking algorithm to identify changes in western disturbance populations between the mid-Holocene and present-day climates for the first time; we will then finish by exploring how these changes play a role in the seasonality of precipitation over the Indus basin and Karakoram.

2 Data

In this study, we make use of outputs from six CMIP5 models - that is all those that have six-hourly output for winds in both the mid-Holocene and historical experiments. These experiments comprise a subset of the Paleoclimate Model Intercomparison Project (PMIP3; Braconnot et al., 2012). Details of those models are given in Tab. 1. Where data availability permits, the table also gives the value of the winter (DJFM) western disturbance frequency bias – indicating whether the historical climatology (1950-2005) of the model produces too many or too few WDs compared to ERA-Interim (which has about 25 per winter, using our tracking algorithm). The models used in this study comprise a fairly representative spread of biases (the multi-model mean bias for all CMIP5 historical models is about +13%, see Hunt et al., 2019), which is important given the resolution sensitivity of WD behaviour in climate models. When combined to assess multi-model means, data are interpolated onto a common, coarse grid.

We use the western disturbance tracking algorithm described in Hunt, Turner, and Shaffrey (2018), tuned for use in CMIP5 GCMs by Hunt et al. (2019). The six-hourly relative vorticity is spectrally truncated at T63 to remove orographic noise and mesoscale eddies, and to provide a common grid between the model outputs. Maxima at 500 hPa are identified and connected using a $k-d$ tree nearest neighbour algorithm (Yianilos, 1993) to form tracks, subject to constraints on propagation speed, track smoothness, and track duration (systems shorter than two days are considered transient). Finally, tracks that are shorter than 48 hours in duration or do not pass eastward through the box 20°N-

Model name	Organisation	$n_x \times n_y$	$\delta_x \times \delta_y$	WWD freq. bias	Reference
bcc-csm1-1*	BCC	128×64	2.81° × 2.79°	+38%	Wu et al. (2013)
CCSM4	NCAR	288×191	1.25° × 0.94°	n/a	Meehl et al. (2012)
CNRM-CM5	CNRM-CERFACS	256×128	1.41° × 1.40°	n/a	Voldoire et al. (2013)
CSIRO-Mk3-6-0*	CSIRO-QCCCE	192×96	1.88° × 1.87°	+44%	Rotstayn et al. (2010)
FGOALS-g2*	LASG-CESS	128×64	2.81° × 2.79°	+4%	L.-J. Li et al. (2013)
FGOALS-s2	LASG-CESS	128×108	2.81° × 1.66°	n/a	L.-J. Li et al. (2013)
GISS-E2-R	NASA-GISS	144×90	2.5° × 2°	n/a	Schmidt et al. (2006)
HadGEM2-CC*	MOHC	192×144	1.88° × 1.25°	+22%	Martin et al. (2011)
HadGEM2-ES	MOHC	192×144	1.88° × 1.25°	n/a	Martin et al. (2011)
IPSL-CM5a-LR*	IPSL	96×95	3.75° × 1.89°	−25%	Dufresne et al. (2013)
MPI-ESM-P*	MPI-M	192×96	1.88° × 1.87°	+35%	Giorgetta et al. (2013)

Table 1. Details of the eleven CMIP5 models used in this study, those marked with an asterisk have six-hourly output and are thus the ones used for tracking. Where available, the bias in winter (DJFM) western disturbance frequency in the model (computed against ERA-Interim) is given.

36.5°N, 60°E-80°E are discarded. Using this domain ensures tracks pass through Pakistan and/or north India and filters out mid-tropospheric cyclones, which are a tropical phenomenon that would otherwise satisfy the tracking criteria. Output tracks are verified against previous case studies to check completeness, and subsequent structure and cluster analysis shows that no secondary systems contaminate the database. The interested reader is encouraged to visit Sec 2.2 of Hunt, Turner, and Shaffrey (2018) for a detailed description of the algorithm.

3 Results

We start by exploring how changes to the upper-tropospheric meridional temperature gradient (UTTG) affect the winter STWJ in mid-Holocene experiments. Fig. 1 shows the change in UTTG between the mid-Holocene and present day, as well as the change in 200 hPa winds, and for illustration the mean location of the STWJ in CMIP5 present-day runs. For consistency throughout, we use the convention that 'change' refers exactly to mid-Holocene minus present day (or control). Here, we choose the UTTG to be pos-

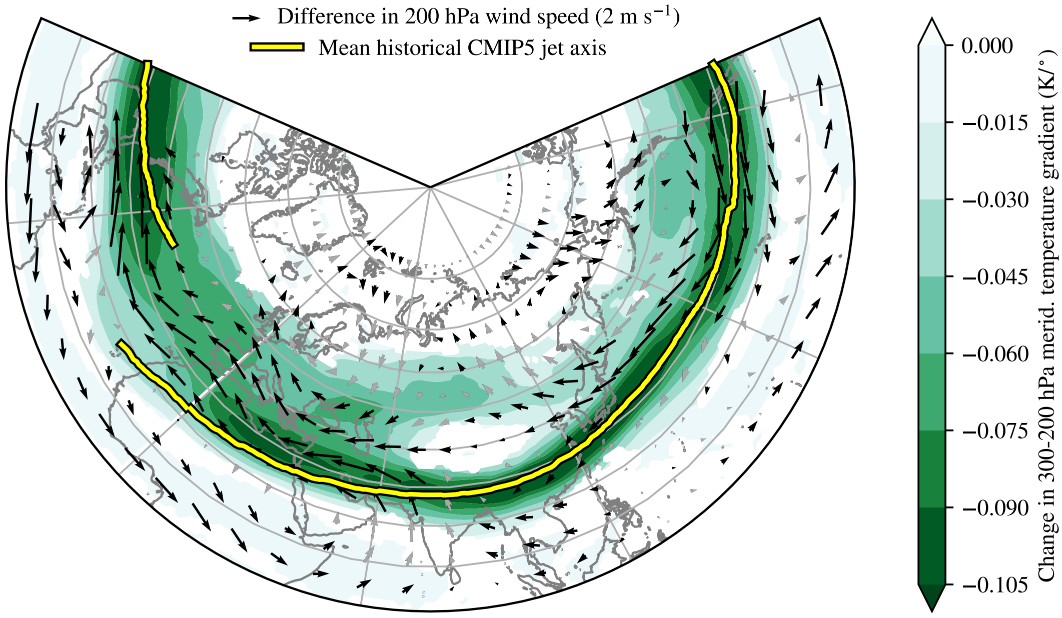

Figure 1. The change (i.e. mid-Holocene minus present day) in DJFM upper level meridional T gradient [K/°], defined as positive when temperature increases in the equatorward direction. Overlaid in quivers are the associated 200 hPa circulation differences, showing retardation and reduced shear of the jet in the MH. Both are computed for the six models in which WD tracking was performed; quivers are grey and contours masked where any model disagrees on the sign of change in zonal wind or temperature gradient change respectively. For reference, the mean present-day CMIP5 jet axis is also shown.

itive (i.e. pole-to-equator gradient, rather than equator to pole), thus the more negative the value is in Fig. 1, the weaker the gradient in the mid-Holocene when compared to present-day.

We see that the expected decline of the UTTG correlates strongly with a weakening of the winter STWJ, particularly along its northern flank. There are two important corollaries: firstly, the smaller temperature gradient, particularly upstream of India, implies that there is less baroclinic instability from which perturbations in the jet can feed off; secondly, the reduction in STWJ strength implies the same for barotropic growth (the relationship between the STWJ and instabilities is discussed in greater detail in Hunt, Curio, et al., 2018).

We hypothesise, therefore, that WDs incident on India during mid-Holocene winters would be weaker and - perhaps - less frequent than the present day. To test this,

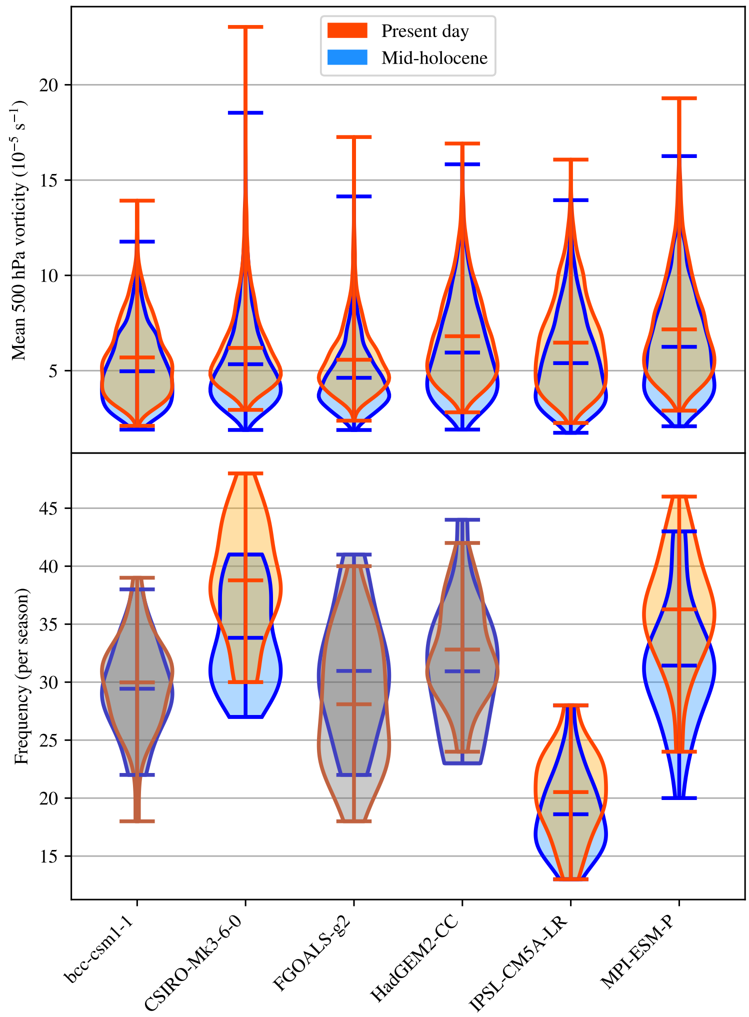

Figure 2. Violin plots indicating the distributions in (top) the seasonal mean western disturbance 500 hPa vorticity and (bottom) the seasonal frequency of DJFM western disturbances for (blue) the mid-Holocene and (orange) the present day, by model. Horizontal lines demarcate minima, means, and maxima respectively. Where the two distributions for a given model are not significantly different from each other, they are greyed out.

an objective tracking algorithm was applied to the six CMIP5/PMIP3 models that had mid-Holocene experiments with six-hourly output (see Table 1), and their present-day counterparts. Statistics for WD frequency and intensity are given for each experiment in Fig. 2, with mid-Holocene in blue and present-day in orange. All experiments record a statistically significant reduction in intensity (defined as the maximum 500 hPa relative vorticity attained between 60°E and 80°E), with the multi-model mean difference amounting to ∼17%; three also record a statistically significant decline in seasonal frequency, with a multi-model mean difference of ∼7% across all six models. Three models do not exhibit a significant change in frequency: bcc-csm1-1, FGOALS-g2, and HadGEM2-CC. Note that the 500 hPa level is chosen as it is the CMIP5 output level closest to the observed centre of WDs (∼ 400 hPa), and that all frequency and intensity analysis is done within the described domain (20-36.5°N, 60-80°E).

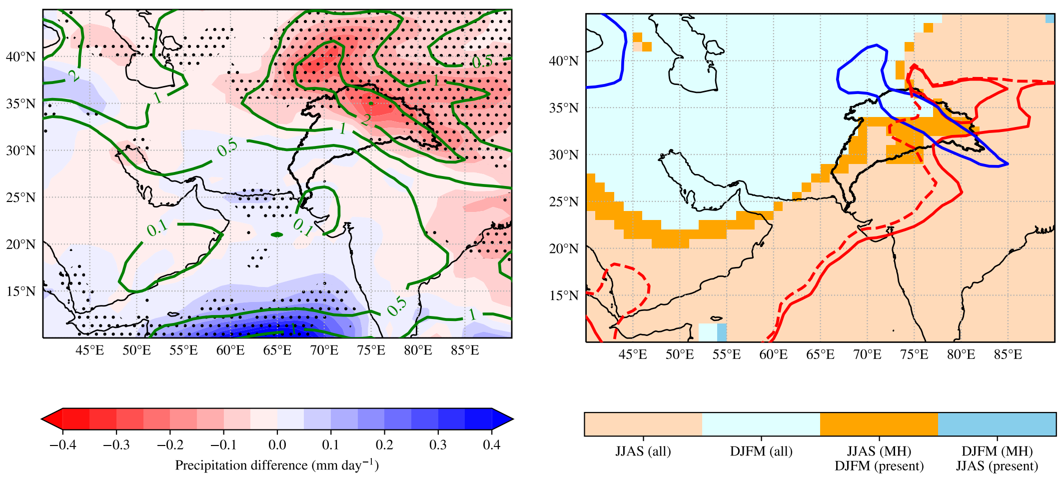

(a) (b)

Figure 3. **(a)** CMIP5 MMM DJFM precipitation [lines, mm day^{-1}] for the historical experiments (in those six models with a mid-Holocene counterpart with six-hourly output) and the difference between mid-Holocene and historical MMM DJFM precipitation [solid, mm day^{-1}]. Stippling indicates where all six models agree on the sign of the change. **(b)** Season of greatest precipitation: light yellow and light teal indicate regions where the season is the same for both MH and historical MMMs (JJAS and DJFM respectively), whereas the dark colours indicate that the seasonality changes (i.e. dark yellow indicates an area where MH precipitation is greatest in JJAS, but historical precipitation peaks in DJFM, and vice versa for dark teal); historical MMM 2 mm day^{-1} isohyets are given for DJFM and JJAS by the dark blue and red lines respectively with mid-Holocene JJAS in dashed red. In both figures, the Indus river basin is marked in solid black.

We have seen that the reduced magnitude of the UTTG in the mid-Holocene both directly (through baroclinic instability of the gradient) and indirectly (through weakening of the STWJ) reduces the frequency and intensity of winter WDs over Pakistan and north India. As previous studies (e.g. Hunt et al., 2019) have indicated, WDs are responsible for almost all winter precipitation in Pakistan, north India, and along much of the Himalayan foothills; so how is mid-Holocene winter precipitation in this region affected by their weakening?

Fig. 3(a) shows the CMIP5 MMM DJFM precipitation climatology (for those models with a MH counterpart experiment), and the change between the MH and the present day. At the head of the Indus basin, where the precipitation is typically the greatest, the mid-Holocene climatology is between 15 and 20% lower than it is in the present day. Transient simulations have shown that the South Asian summer monsoon was both stronger and had greater extent during the mid-Holocene period (Liu et al., 2004), which agrees with pollen records where available (Lézine, Ivory, Braconnot, & Marti, 2017). Fig. 3(b) compares the winter (DJFM) and summer (JJAS) climatologies for both the historical and mid-Holocene period, indicating the regions in which both or neither dominate the seasonal cycle. The dividing line between winter-dominant (i.e., DJFM) and summer-dominant (i.e., JJAS) precipitation regions retreats southeastward as the mid-Holocene finishes and the extent of the summer monsoon starts to decline. This effect is exaggerated considerably along the Karakoram (the mountain range spanning north Pakistan and north India) as the winter precipitation also increases as a result of the previous described changes in WD activity. Fig. S1 shows how the seasonal cycle of precipitation changes in the basin between the two epochs. Supporting Fig. 3(b), it shows a well defined boreal summer peak in the mid-Holocene, which moves to a winter-spring peak in the present day. Fourier decomposition (e.g. Dwyer, Biasutti, & Sobel, 2012) reveals that the two cycles have significantly different phase and amplitude. The result from the point of view of the Indus basin is thus twofold: a shift of primary growing season from summer (in the mid-Holocene, e.g. Dave, Courty, Fitzsimmons, & Singhvi, 2018; Giosan et al., 2012) to winter (in the present day, Kalra et al., 2008; Sarker & Quaddus, 2002); and a shift in the location of the area of peak precipitation, from the east and northeast of the basin to the orographic band in the north. Each feature of Fig. 3(a) and Fig. 3(b) discussed in this section persist when the analysis is done with all eleven mid-Holocene models. As discussed in the introduction, there is a dearth of winter/seasonal paleoclimate reconstructions in the Indus basin; however, a number have looked at proxies in the northwest Himalaya, a region bordering the north/northeast of our domain. Both pollen (Demske, Tarasov, Wünnemann, & Riedel, 2009) and sediment (Prasad & Enzel, 2006) records indicate a period of reduced winter precipitation 6 ka before present.

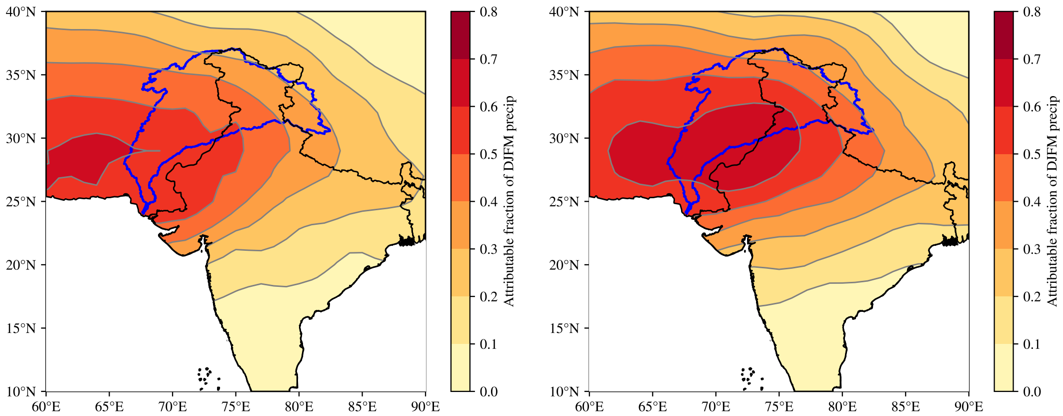

(a) mid-Holocene (b) present-day

Figure 4. Fraction of the climatological winter precipitation attributed to western disturbance activity in (a) mid-Holocene and (b) historical CMIP5 experiments, computed in each case using the six models for which six-hourly mid-Holocene output is available. Precipitation is attributed if it occurs within 800 km and 24 hours of a passing WD. The catchment boundary of the Indus basin is marked in blue.

To complete our argument, we must determine whether the change in WDs is responsible for the change in precipitation. To do that, we can compare the fraction of winter precipitation caused by western disturbances in the mid-Holocene to the present day. Fig 4 shows that there is a roughly uniform increase of about 0.1 in the fraction of attributed precipitation across the Indus basin from the mid-Holocene to the present-day. This follows the fractional change seen in Fig. 3(a), and provides strong evidence that increasing winter rainfall in the region after the mid-Holocene was caused by increased WD activity.

4 Discussion

In this study, we have explored how changes in orbital parameters between the mid-Holocene period (MH; 7-5 ka) and the present day affect the boreal winter subtropical westerly jet and its impacts on storms known as western disturbances (WDs) which affect northern India and Pakistan. Orbital precession resulted in a more pronounced global seasonal cycle and acted to reduce the upper-tropospheric meridional temperature gradient in boreal winter. We have shown that this reduction in gradient weakens the northern flank of the subtropical westerly jet, which previous studies (Hunt, Curio, et al., 2018) have shown result in less baroclinic and barotropic instability for WDs when they reach India - to feed off. This resulted in mid-Holocene South Asia being impacted by weaker and less frequent WDs. All six models used in this study agreed that WD intensity was significantly lower during the mid-Holocene, though a significant decline in WD frequency was found in only three.

Since WDs are very strongly tied to winter rainfall over Pakistan and northern India (where they are typically responsible for about 70% of present day winter precipitation), the reduced activity during the mid-Holocene resulted in a decline of about 15% in winter precipitation at the head of the Indus basin. Previous studies have shown that the South Asian summer monsoon was stronger and had a greater northwestward extent during the mid-Holocene; combined with the previous result, this has a profound impact on the Indus river basin. There, in the mid-Holocene, most precipitation fell during the summer monsoon, focused in the east; instead in the present day, most precipitation falls during the winter, and tends to be focused in the north, along the orography.

This change in growing season is complementary to previous explanations for the collapse of the Harappan Civilisation, which underwent agricultural failure and eastward migration towards the end of the mid-Holocene period. We hope that further work, in particular the discovery of robust proxies for winter precipitation in the region, will continue to explore this problem in more detail.

Acknowledgments

This study was supported by the JPI-Climate and Belmont Forum Climate Predictability and Inter-Regional Linkages Collaborative Research Action via NERC grant NE/P006795/1. We acknowledge the World Climate Research Programme's Working Group on Coupled Modelling,which is responsible for CMIP (`http://pcmdi9.llnl.gov`), and we thank the climate modeling groups for producing and making available their model output. For CMIP the U.S. Department of Energy's Program for Climate Model Diagnosis and Intercomparison provides coordinating support and led development of software infrastructure in partnership with the Global Organization for Earth System Science Portals. ERA-Interim reanalysis data are available from ECMWF at `https://www.ecmwf.int/en/forecasts/datasets/reanalysis-datasets/era-interim`. The tracking algorithm used is available from the first author. Track datasets for ERA-Interim and CMIP5 experiments are available from the BADC at `https://catalogue.ceda.ac.uk/uuid/b1f266c25cf2445f8b87d874f6ac830a`.

The authors wish to thank three anonymous reviewers for constructive comments on our manuscript.

References

Berkelhammer, M., Sinha, A., Stott, L., Cheng, H., Pausata, F. S., Yoshimura, K., et al. (2012). An abrupt shift in the Indian monsoon 4000 years ago. *Geophys. Monogr. Ser*, *198*(7).

Bosmans, J. H. C., Drijfhout, S. S., Tuenter, E., Lourens, L. J., Hilgen, F. J., & Weber, S. L. (2012). Monsoonal response to mid-holocene orbital forcing in a high resolution gcm. *Climate of the Past*, *8*(2), 723–740.

Braconnot, P., Harrison, S. P., Kageyama, M., Bartlein, P. J., Masson-Delmotte, V., Abe-Ouchi, A., ... Zhao, Y. (2012). Evaluation of climate models using palaeoclimatic data. *Nature Climate Change*, *2*(6), 417.

Braconnot, P., Loutre, M., Dong, B., Joussaume, S., Valdes, P., et al. (2002). How the simulated change in monsoon at 6 ka BP is related to the simulation of the modern climate: results from the Paleoclimate Modeling Intercomparison Project. *Climate Dynamics*, *19*(2), 107–121.

Braconnot, P., Otto-Bliesner, B., Harrison, S., Joussaume, S., Peterchmitt, J.-Y., Abe-Ouchi, A., ... others (2007). Results of PMIP2 coupled simulations of the Mid-Holocene and Last Glacial Maximum–Part 1: experiments and large-scale features. *Climate of the Past*, *3*(2), 261–277.

Bryson, R. A. (1992). A macrophysical model of the holocene intertropical convergence and jetstream positions and rainfall for the saharan region. *Meteorology and Atmospheric Physics*, *47*(2-4), 247–258.

Bryson, R. A. (1997). Proxy indications of Holocene winter rains in southwest Asia compared with simulated rainfall. In *Third millennium bc climate change and old world collapse* (pp. 465–473). Springer.

Bryson, R. A., & Swain, A. M. (1981). Holocene variations of monsoon rainfall in Rajasthan. *Quaternary Research*, *16*(2), 135–145.

Dave, A. K., Courty, M.-A., Fitzsimmons, K. E., & Singhvi, A. K. (2018). Revisiting the contemporaneity of a mighty river and the Harappans: Archaeological, stratigraphic and chronometric constraints. *Quaternary Geochronology*, *49*, 230–235.

Demske, D., Tarasov, P. E., Wünnemann, B., & Riedel, F. (2009). Late glacial and holocene vegetation, Indian monsoon and westerly circulation in the Trans-Himalaya recorded in the lacustrine pollen sequence from Tso Kar, Ladakh, NW India. *Palaeogeography, Palaeoclimatology, Palaeoecology*, *279*(3), 172–185.

Dikshit, K. N. (1979). Old channels of Ghaggar in Rajasthan-revisited. *Man and Environment*, *3*, 105–106.

Dufresne, J.-L., Foujols, M.-A., Denvil, S., Caubel, A., Marti, O., Aumont, O., ... others (2013). Climate change projections using the IPSL-CM5 Earth System Model: from CMIP3 to CMIP5. *Climate Dynamics*, *40*(9-10), 2123–2165.

Dwyer, J. G., Biasutti, M., & Sobel, A. H. (2012). Projected changes in the seasonal cycle of surface temperature. *Journal of Climate*, *25*(18), 6359–6374.

Flam, L. (2002). Fluvial geomorphology of the lower Indus basin (Sindh, Pakistan) and the Indus civilization. In *Himalaya to the sea* (pp. 186–200). Routledge.

Giorgetta, M. A., Jungclaus, J., Reick, C. H., Legutke, S., Bader, J., Böttinger, M., ... others (2013). Climate and carbon cycle changes from 1850 to 2100 in MPI-ESM simulations for the Coupled Model Intercomparison Project phase 5. *Journal of Advances in Modeling Earth Systems*, *5*(3), 572–597.

Giosan, L., Clift, P. D., Macklin, M. G., Fuller, D. Q., Constantinescu, S., Durcan, J. A., ... others (2012). Fluvial landscapes of the harappan civilization. *Proceedings of the National Academy of Sciences*, *109*(26), E1688–E1694.

Harrison, S. P., Kutzbach, J. E., Liu, Z., Bartlein, P. J., Otto-Bliesner, B., Muhs, D., ... Thompson, R. S. (2003). Mid-holocene climates of the Americas: a dynamical response to changed seasonality. *Climate Dynamics*, *20*(7-8), 663–688.

Hou, J., D'Andrea, W. J., Wang, M., He, Y., & Liang, J. (2017). Influence of the Indian monsoon and the subtropical jet on climate change on the Tibetan Plateau since the late Pleistocene. *Quaternary Science Reviews*, *163*, 84–94.

Hunt, K. M. R., Curio, J., Turner, A. G., & Schiemann, R. (2018). Subtropical westerly jet influence on occurrence of western disturbances and tibetan plateau vortices. *Geophysical Research Letters*, *45*(16), 8629–8636.

Hunt, K. M. R., Turner, A. G., & Shaffrey, L. C. (2018). The evolution, seasonality, and impacts of western disturbances. *Quart. J. Roy. Meteor. Soc.*, *144*(710), 278–290. doi: 10.1002/qj.3200

Hunt, K. M. R., Turner, A. G., & Shaffrey, L. C. (2019). Representation of western disturbances in CMIP5 models. *J. Climate*. (In press) doi: 10.1175/JCLI-D-18-0420.1

Joussaume, S., Taylor, K. E., Braconnot, P. J. F. B., Mitchell, J. F. B., Kutzbach, J. E., Harrison, S. P., ... others (1999). Monsoon changes for 6000 years ago: results of 18 simulations from the Paleoclimate Modeling Intercomparison Project (PMIP). *Geophysical Research Letters*, *26*(7), 859–862.

Kalra, N., Chakraborty, D., Sharma, A., Rai, H. K., Jolly, M., Chander, S., ... others (2008). Effect of increasing temperature on yield of some winter crops in northwest India. *Current Science*, 82–88.

Krishnamurti, T. N. (1961). The subtropical jet stream of winter. *Journal of Meteorology*, *18*(2), 172–191.

Lézine, A.-M., Ivory, S. J., Braconnot, P., & Marti, O. (2017). Timing of the southward retreat of the ITCZ at the end of the Holocene Humid Period in Southern Arabia: Data-model comparison. *Quaternary Science Reviews*, *164*, 68–76.

Li, J., Ehlers, T. A., Werner, M., Mutz, S. G., Steger, C., & Paeth, H. (2017). Late quaternary climate, precipitation δ18o, and indian monsoon variations over the Tibetan Plateau. *Earth and Planetary Science Letters*, *457*, 412–422.

Li, L.-J., Lin, P.-F., Yu, Y.-Q., Wang, B., Zhou, T.-J., Liu, L., ... others (2013). The flexible global ocean-atmosphere-land system model, Grid-point Version 2: FGOALS-g2. *Advances in Atmospheric Sciences*, *30*(3), 543–560.

Liu, Z., Harrison, S. P., Kutzbach, J., & Otto-Bliesner, B. (2004). Global monsoons in the mid-Holocene and oceanic feedback. *Climate Dynamics*, *22*(2-3), 157–182.

Madella, M., & Fuller, D. Q. (2006). Palaeoecology and the Harappan civilisation of South Asia: a reconsideration. *Quaternary Science Reviews*, *25*(11-12), 1283–1301.

Martin, G. M., Bellouin, N., Collins, W. J., Culverwell, I. D., Halloran, P. R., Hardiman, S. C., ... others (2011). The HadGEM2 family of Met Office Unified

Model climate configurations. *Geoscientific Model Development*, *4*(3), 723–757.

Martyn, D. (2002). Climates of the world. In *Developments ion atmospheric science* (pp. 389–400). Elsevier.

Meehl, G. A., Washington, W. M., Arblaster, J. M., Hu, A., Teng, H., Tebaldi, C., … others (2012). Climate system response to external forcings and climate change projections in CCSM4. *Journal of Climate*, *25*(11), 3661–3683.

Misra, V. N. (1984). Climate, a factor in the rise and fall of the Indus Civilization-Evidence from Rajasthan and beyond. In M. Rangarajan (Ed.), *Environmental issues in india, a reader* (pp. 461–490). Pearson.

Palazzi, E., Hardenberg, J., & Provenzale, A. (2013). Precipitation in the Hindu-Kush Karakoram Himalaya: Observations and future scenarios. *J. Geophys. Res. Atmos.*, *118*(1), 85–100.

Palazzi, E., von Hardenberg, J., Terzago, S., & Provenzale, A. (2015). Precipitation in the Karakoram-Himalaya: a CMIP5 view. *Climate Dyn.*, *45*(1-2), 21–45.

Pant, G. B., & Maliekal, J. A. (1987). Holocene climatic changes over northwest India: An appraisal. *Climatic Change*, *10*(2), 183–194.

Possehl, G. L. (1997a). Climate and the eclipse of the ancient cities of the Indus. In *Third millennium bc climate change and old world collapse* (pp. 193–243). Springer.

Possehl, G. L. (1997b). The transformation of the Indus civilization. *Journal of World Prehistory*, *11*(4), 425–472.

Prasad, S., & Enzel, Y. (2006). Holocene paleoclimates of india. *Quaternary Research*, *66*(3), 442–453.

Raikes, R. L., & Dales, G. F. (1986). Reposte to Wasson's sedimentological basis of the Mohenjo-Daro flood hypothesis. *Man and Environment*, *10*, 33–44.

Raikes, R. L., & Dyson, R. H. (1961). The prehistoric climate of Baluchistan and the Indus Valley. *American Anthropologist*, *63*(2), 265–281.

Rawat, S., Gupta, A. K., Srivastava, P., Sangode, S., & Nainwal, H. (2015). A 13,000 year record of environmental magnetic variations in the lake and peat deposits from the Chandra valley, Lahaul: Implications to Holocene monsoonal variability in the NW Himalaya. *Palaeogeography, palaeoclimatology, palaeoecology*, *440*, 116–127.

Rotstayn, L. D., Collier, M. A., Dix, M. R., Feng, Y., Gordon, H. B., O'Farrell, S. P., ... Syktus, J. (2010). Improved simulation of Australian climate and ENSO-related rainfall variability in a global climate model with an interactive aerosol treatment. *International Journal of Climatology*, *30*(7), 1067–1088.

Sarker, R. A., & Quaddus, M. A. (2002). Modelling a nationwide crop planning problem using a multiple criteria decision making tool. *Computers & Industrial Engineering*, *42*(2-4), 541–553.

Schiemann, R., Lüthi, D., & Schär, C. (2009). Seasonality and interannual variability of the westerly jet in the Tibetan Plateau region. *J. Climate*, *22*(11), 2940–2957.

Schmidt, G. A., Ruedy, R., Hansen, J. E., Aleinov, I., Bell, N., Bauer, M., ... others (2006). Present-day atmospheric simulations using GISS ModelE: Comparison to in situ, satellite, and reanalysis data. *Journal of Climate*, *19*(2), 153–192.

Staubwasser, M., Sirocko, F., Grootes, P. M., & Segl, M. (2003). Climate change at the 4.2 ka BP termination of the Indus valley civilization and Holocene south Asian monsoon variability. *Geophysical Research Letters*, *30*(8).

Syed, F. S., Giorgi, F., Pal, J. S., & King, M. P. (2006). Effect of remote forcings on the winter precipitation of central southwest Asia part 1: observations. *Theoretical and Applied Climatology*, *86*(1-4), 147–160.

Voldoire, A., Sanchez-Gomez, E., y Mélia, D. S., Decharme, B., Cassou, C., Sénési, S., ... others (2013). The CNRM-CM5.1 global climate model: description and basic evaluation. *Climate Dynamics*, *40*(9-10), 2091–2121.

Wei, J., & Wang, H. (2004). A possible role of solar radiation and ocean in the mid-Holocene East Asian monsoon climate. *Advances in Atmospheric Sciences*, *21*(1), 1–12.

Wu, T., Li, W., Ji, J., Xin, X., Li, L., Wang, Z., ... others (2013). Global carbon budgets simulated by the Beijing Climate Center Climate System Model for the last century. *Journal of Geophysical Research: Atmospheres*, *118*(10), 4326–4347.

Yianilos, P. N. (1993). Data structures and algorithms for nearest neighbor search in general metric spaces. In *Soda* (Vol. 93, pp. 311–21).

You, Q.-L., Ren, G.-Y., Zhang, Y.-Q., Ren, Y.-Y., Sun, X.-B., Zhan, Y.-J., ... Krishnan, R. (2017). An overview of studies of observed climate change in the

Hindu Kush Himalayan (HKH) region. *Advances in Climate Change Research*, *8*(3), 141–147.